Translational Oncology
www.transonc.com

Volume 10 Number 5 October 2017 pp. 786–792 786

Association Between Background Parenchymal Enhancement and Pathologic Complete Remission Throughout the Neoadjuvant Chemotherapy in Breast Cancer Patients

Chao You*, Weijun Peng*, Wenxiang Zhi†, Min He‡, Guangyu Liu‡, Li Xie§, Luan Jiang¶, Xiaoxin Hu*, Xuxia Shen# and Yajia Gu*

*Department of Radiology, Fudan University Cancer Center, Department of Oncology, Shanghai Medical College, Fudan University, Shanghai, PR China; †Department of Ultrasound, Fudan University Cancer Center, Department of Oncology, Shanghai Medical College, Fudan University, Shanghai, PR China; ‡Department of Breast Surgery, Key Laboratory of Breast Cancer in Shanghai, Fudan University Shanghai Cancer Center, Department of Oncology, Shanghai Medical College, Fudan University, Shanghai, PR China; §Statistical Office, Fudan University Cancer Center, Department of Oncology, Shanghai Medical College, Fudan University, Shanghai, PR China; ¶Center for Advanced Medical Imaging Technology, Shanghai Advanced Research Institute, Chinese Academy of Sciences, Shanghai, PR China; #Department of Pathology, Fudan University Shanghai Cancer Center, Department of Oncology, Shanghai Medical College, Fudan University Shanghai, PR China

Abstract

PURPOSE: To retrospectively investigate the quantitative background parenchymal enhancement (BPE) of the contralateral normal breast in patients with unilateral invasive breast cancer throughout multiple monitoring points of neoadjuvant chemotherapy (NAC) and to further determine whether BPE is associated with tumor response, especially at the early stage of NAC. *MATERIALS AND METHODS:* A total of 90 patients with unilateral breast cancer who then received six or eight cycles of NAC before surgery were analyzed retrospectively. BPE was measured in dynamic contrast-enhanced MRI at baseline and after 2nd, 4th, and 6th NAC, respectively. Correlation between BPE and tumor size was analyzed, and the association between pathologic complete remission (pCR) and BPE was also analyzed. *RESULTS:* The BPE of contralateral normal breast showed a constant reduction throughout NAC therapy regardless of the menopausal status ($P < .001$ in all). Both the BPEs and the changes of BPE in each of the three monitoring points were significantly correlated with those in tumor size ($P < .05$ in all), and the reduction of BPE after 2nd NAC had the largest diagnostic value for pCR (AUC = 0.726, $P < .001$), particularly in hormonal receptor (HR)-negative patients (OR = 0.243, 95%CI = 0.083 to 0.706, $P = .009$). *CONCLUSION:* The BPE of contralateral normal breast had a constant decreased tendency similar to the change of tumor size in NAC. Reduction of BPE at the early stage of NAC was positively associated with pCR, especially in HR-negative status.

Translational Oncology (2017) 10, 786–792

Introduction

Breast background parenchymal enhancement (BPE) is referred to as normal fibroglandular breast tissue enhancement on the MR mammography (MRM) after injecting contrast agents, which is known to be evaluated qualitatively according to the BI-RADS lexicon or measured quantitatively by a fully automated computerized

Address all correspondence to: YaJia Gu, MD, Department of Radiology, Fudan University Cancer Center, Department of Oncology, Shanghai Medical College, Fudan University, No 270, Dongan Road, 200032, Shanghai, China.
E-mail: cjr.guyajia@vip.163.com
Received 10 July 2017; Revised 20 July 2017; Accepted 24 July 2017

1936-5233/17
http://dx.doi.org/10.1016/j.tranon.2017.07.005

scheme [1,2]. Since BPE is thought to coincide with the amount of blood flow in the fibroglandular tissue and may reflect breast activity, there are many studies that demonstrated that BPE was associated with fibroglandular tissue (FGT), patient's age, menopausal status, and menstrual phase [3–6].

Previous studies have investigated the influence of BPE on the affected breast harboring breast cancer. It was proposed that increased levels of BPE are an important risk factor for breast cancer [3,7,8]. It was revealed that moderate or marked BPE surrounding breast tumors may affect the accuracy of the tumor size estimation, leading to a positive resection margin after breast conservation surgery [9].

In addition, higher BPE around the tumor at preoperative MR imaging could be an independent factor associated with worse recurrence-free survival in patients with ductal carcinoma in suit (DCIS) [10,11]. Besides surgery treatment, it was also previously demonstrated that other well established treatments, such as radiation, chemotherapy and antihormonal medications were also associated with BPE [7,12–14]. The reductions of BPE may have been caused by any other therapies or by their combination.

A few of studies recently have focused on the association between BPE and tumor outcome to neoadjuvant chemotherapy (NAC). Preibsch et al. demonstrated that the decreased BPE after NAC seemed to correlate with tumor response by using qualitative analysis [15]. Given the typical symmetry between left and right breast, Chen et al. and van der Velden et al., respectively, investigated the alternation of BPE in the contralateral normal breast by using fully automated computerized method [16,17]. Chen et al. found that a reduction of BPE was associated with pathologic complete remission (pCR) to NAC in estrogen receptor (ER)*negative patients, while van der Velden et al. revealed that the association between BPE and long-term outcome was significant particularly in patients with ER-positive and human epidermal growth factor receptor 2 (HER2)-negative breast cancers. Although these studies confirmed that the alternation of BPE can predict tumor outcome in NAC, they have not reached an agreement on different subtypes according to immunohistochemistry (IHC). Additionally, some of the published studies ignored the fact to unify the observation point of BPE after NAC, and some of them aimed for a change of BPE before the surgery just after completing NAC. None of them focused on the change of BPE at every time point throughout NAC in breast patients.

Thus, the purpose of this retrospective study was to quantify BPE in breast cancer patients throughout different time points during NAC and further to determine whether quantitative MR imaging assessments of BPE in the contralateral normal breast are associated with tumor response, especially at the early stage of NAC.

Materials and Methods

Patient Enrollment

The institutional review board granted a waiver of authorization and patient consent for our retrospective study, which was in compliance with the Health Insurance Portability and Accountability Act (HIPAA). Between August 2014 and April 2016, 116 patients diagnosed with breast cancers were confirmed by core needle biopsy, and received six or eight cycles of neoadjuvant chemotherapy (NAC). Diagnosis of suspicious axillary lymph node was confirmed by ultrasound-guided fine-needle aspiration. Altogether, 26 patients were excluded — among them 10 did not receive surgery after NAC, 5 had bilateral breast cancers, and 11 had insufficient MRI data. Finally, 90 patients (mean age ± SD, 49.84 ± 10.04 years; age range, 28–69 years) with unilateral breast cancer (72 invasive ductal carcinomas, 5 ductal carcinoma in suit, 2 invasive lobular carcinoma and 11 tumor classification unclear) were included in our study. Menopausal status was recorded in medical history, then patients were separated into pre-menopausal (mean age ± SD, 40.88 ± 6.55 years, N = 50) and post-menopausal groups ((mean age ± SD, 57.02 ± 5.55, N = 40). Among them, all patients underwent contrast-enhanced breast MRI before and after NAC.

NAC Protocol

The NAC regimens included CEF (cyclophosphamide 600 mg/m^2 on day 1, epirubicin 60 mg/m^2 on day 1 and 5-fluorouracil 600 mg/m^2 on day 1 every 3 weeks), PC (paclitaxel 80 mg/m^2 and carboplatin AUC 2 mg min/ml on days 1, 8, and 15 of a 28-day cycle) and PE (paclitaxel, 80 mg/m^2 on Days 1, 8, and 15, epirubicin 60 mg/m^2 on day 1 every 3 weeks) for a median of 4 cycles (range 1 to 6 cycles). TEC (Taxotere 75 mg/m^2, epirubicin 60 mg/m^2 cyclophosphamide 600 mg/m^2 on day 1 of a 21-day cycle). For HER-2 positive patients, Trastuzumab was administered as 4 mg/kg loading dose followed by 2 mg/kg weekly combined with chemotherapy (PCH). Breast surgery with axillary dissection was performed within 4 weeks at the last chemotherapy dose for all the patients. In total, 5 patients received CEF, 20 patients received PC, 2 cases underwent PE, 29 cases underwent TEC and 39 patients received PCH.

MRI Study Protocol

MRI was performed with 1.5-T Dedicated spiral breast MRI Systems (Aurora Imaging Technology, Aurora Systems, Inc., Canada) with breast coil. The patient was prone, and images were acquired in the axial planes with the following sequences: a T2-weighted fat-suppressed sequence (TR 6680 ms, TE 29 ms, thickness 3 mm), and axial T1-weighted fat suppressed (TE/TR 4.8/29 ms, thickness 1.1 mm, FOV 360 mm, matrix 360 × 360 × 128) before and four times after a bolus injection of gadopentetate dimeglumine at 2 ml/s with an injector and followed by 20 ml normal saline flush. Postcontrast images were obtained at 90, 180, 270, and 360 seconds after injection. The same acquisition parameters were used throughout NAC studies. The baseline MRI scans were scheduled prior to initiation of NAC, at least 10 days after biopsy. The follow-up MRI scans were usually scheduled after the 2nd, 4th, 6th, and 8th cycle of NAC just before commencing the next cycle, respectively. Only 12 patients received eight cycles of NAC; therefore, the data of 8th follow-up MRI were excluded in this study.

Histopathological Analysis

Prior to NAC, biopsy of the primary tumor was taken for histological analysis. Pathologic tumor response was assessed by the Miller and Payne grading [18]. pCR in the breast was defined as the absence of invasive carcinoma (residual ductal carcinoma in situ allowed) by pathologic examination.

Image Processing

We developed a fully automated scheme for the quantitative analysis of BPE in DCE-MRI. It has been used in our previous study [19]. Our fully automated method consists of three steps, segmentation of the whole breast, fibroglandular tissues, and enhanced fibroglandular tissues. Based on the volume of interest

extracted, dynamic programming technique was applied in each 2-D slice of the 3-D MR scan to delineate the chest wall and breast skin line for segmenting the whole breast. This step took advantage of the continuity of the chest wall and breast skin line across adjacent slices. We then further used the fuzzy c-means clustering method with an automatic selection of cluster numbers for segmenting the fibroglandular tissues within the segmented whole breast area. Finally, a statistical method was used to set a threshold based on the estimated noise level for segmenting the enhanced fibroglandular tissues in the subtraction image of pre- and post-contrast MRI scans (Figure 1). BPE was calculated with the segmented volumes of the enhanced fibroglandular tissues and the fibroglandular tissues. BPE = (the enhanced fibroglandular tissue volume/total fibroglandular tissue volume) × 100%. To avoid the effects of the lesion, only BPE of the contralateral normal breast was evaluated. BPE was measured on four time points, respectively, and calculated the mean value as statistic data.

Data Analysis

Since monitoring tumor response to NAC is universally accepted by Response Evaluation Criteria in Solid Tumors (RECIST) [20], tumor size was also analyzed in this study, which was measured on early post-contrast images (90 seconds after contrast material injection).

The changes in BPE between four MRIs were calculated according to the following formula: $\Delta BPE_{1/2/3}$ = ($BPE_{2nd/4th/6th\ follow\text{-}up\ MRI}$ − $BPE_{baseline\ MRI}$)/$BPE_{baseline\ MRI}$ *100%. Reduction of the tumor size on post-NAC MRI was calculated as follows: $\Delta Size_{1/2/3}$ = (tumor $size_{2nd/4th/6th\ follow\text{-}up\ MRI}$ − tumor $size_{baseline\ MRI}$)/tumor $size_{baseline\ MRI}$ *100%.

Statistical Analysis

All data was analyzed using the SPSS 16.0 software. The Independent *t* test and Pearson chi-square test were used to compare baseline characteristics in pCR and Non-pCR Groups. The Nonparametric test was used to compare BPEs throughout the NAC. Correlation between Δ BPE and Δ size was analyzed using Spearman's test. Association between pCR and other variables was analyzed by Binary Logistic regression. The predictive performance regarding the identification of responders or nonresponders was evaluated by ROC analysis. $P < .05$ was considered statistically significant.

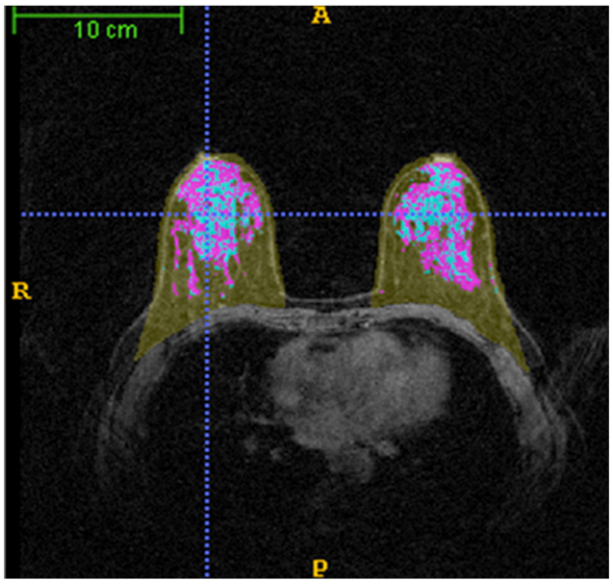

Figure 1. Magnetic resonance imaging analysis.The volume of interest (VOI) of breasts, yellow color for the whole breast, blue for the fibroglandular tissue without enhancement and pink for the enhanced fibroglandular tissue.

Results

Patient Cohort and Tumor Characteristics

The baseline characteristics of the study population are shown in Table 1. After completing NAC, there were 25 patients (27.78%) who received pCR, and 65 cases received non-pCR (72.22%). The proportions of IHC type, hormonal receptor (HR) status and HER2 status were significantly different between pCR and non-pCR groups.

BPE and NAC

Compared with baseline status, BPE after 2nd, 4th, and 6th NAC showed a significant reduction in all the patients ($P < .001$ in all). Forty patients were pre-menopausal and 50 patients were post-menopausal at the time of baseline MRI. Regardless of menopausal status, they had a similar trend throughout NAC. The reduction of BPE was less in post-menopausal women than that in pre-menopausal women in all the three monitoring points, but it did not reach a significant difference (Figure 2).

BPE and Tumor Size

No significant correlation was seen between BPE and tumor size (r = 0.024, $P = .825$) at baseline, while the correlation became a weak but significant after NAC during each of three monitoring points (r = 0.286, $P = .006$ after 2nd NAC, r = 0.266, $P = .011$

Table 1. Baseline Characteristics of the Patient Cohort in the pCR and non-pCR Groups

Characteristics	Total (n = 90)	pCR (n = 25)	Non-pCR (n = 65)	*P*
Age (mean year ± SD)	49.84 ± 10.04	48.76 ± 10.68	50.26 ± 9.84	.722
Tumor size (mm)	40.66 ± 14.20	41.64 ± 14.85	40.28 ± 14.04	.538
Tumor size group				.422
≤20 mm	4 (4.45)	2 (8)	2 (3.08)	
21-50 mm	65 (72.22)	16 (64)	49 (75.38)	
>50 mm	21 (23.33)	7 (28)	14 (21.54)	
Menopausal status				.813
Pre-menopausal	50 (55.56)	13 (52)	37 (56.92)	
Post-menopausal	40 (44.44)	12 (48)	28 (43.08)	
Histopathological type				.054
IDC	72 (80)	11 (44)	61 (93.84)	
DCIS	5 (5.56)	3 (12)	2 (3.08)	
ILC	2 (2.22)	1 (4)	1 (1.54)	
Unclear classification	11 (12.22)	10 (40)	1 (1.54)	
Immunohistochemistry type				.020*
Luminal A	9 (10)	2 (8)	7 (10.77)	
Luminal B	27 (30)	2 (8)	25 (38.46)	
HER2 positive	35 (38.89)	15 (60)	20 (30.77)	
Triple negative	19 (21.11)	6 (24)	13 (20)	
HR status				.015*
ER/PR(−)	32 (35.56)	14 (56)	18 (27.69)	
ER/PR(+)	58 (64.44)	11 (44)	47 (72.31)	
HER2 status				.018*
HER2 (−)	51 (56.67)	9 (36)	42 (64.62)	
HER2 (+)	39 (43.33)	16 (64)	23 (35.38)	
Lymph node				.770
negative	18 (20)	4 (16)	14 (21.54)	
Positive	72 (80)	21 (84)	51 (78.46)	

Abbreviations: IDC, invasive ductal carcinoma; ILC, invasive lobular carcinoma; pCR, pathologic complete response; HR, hormonal receptor; ER, estrogen receptor; PR, progesterone receptor; HER2, human epidermal growth factor receptor. Numeric data are presented as mean ± SD. Nonnumeric data are presented as number of patients (percentage). *P* value was analyzed between pCR group and non-pCR group.

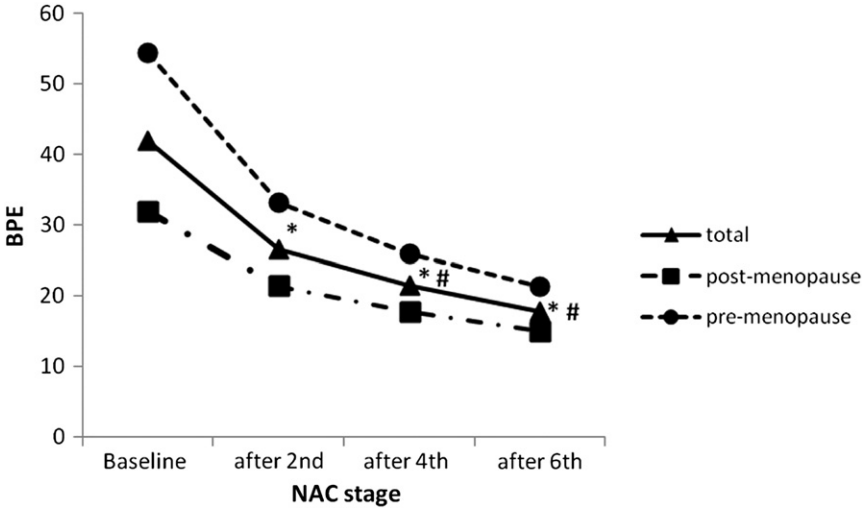

Figure 2. Line graph displays average value of background parenchymal enhancement (BPE) in all the patients, pre- and post-menopausal women. Note: * $P < .001$ compared with baseline. # $P < .001$ compared with the previous NAC stage.

after 4th NAC, and r = 0.235, $P = .026$ after 6th NAC). Meanwhile, we also found that there was a weak significant correlation between the decrease of BPE and the reduction of tumor size in each of three observation points during NAC (r = 0.373, $P < .001$ after 2nd NAC, r = 0.249, $P = .018$ after 4th NAC, and r = 0.264, $P = .012$ after 6th NAC).

The Cut-Off Point of BPE for pCR

The diagnostic values of Δ BPE and Δ size for pCR were further analyzed with ROC curve (Figures 3, 4). The AUC of ΔBPE was largest after 2nd NAC and the AUC of Δsize was largest after 6th NAC. After 2nd NAC, the AUC of ΔBPE was 0.726 and the cut-off point between pCR and non-pCR groups was 0.2672 (sensitivity 88% and specificity 52.3%), while the AUC of Δsize was 0.704 and the cut-off point for pCR was 0.3258 (sensitivity 80% and specificity 61.5%) (Table 2).

Association Analysis

In univariate analysis, decrease of BPE was positively correlated with pCR in the three monitoring points during NAC ($P = .002$ for 2nd NAC, 0.007 for 4th NAC and 0.036 for 6th NAC, respectively). Meanwhile, the reduction of tumor size were also significantly positively associated with pCR in every observation point ($P = .004$ for 2nd NAC and $P < .001$ for both 4th and 6th NAC). The HR status and HER2 status showed significant associations with pCR ($P = .014$ and 0.016, respectively). There were no associations between pCR and age, menopausal status, tumor size at baseline and lymph mode status ($P > .05$). Variables showing a significant association with pCR in univariate analysis were entered for multivariate analysis stratified to three monitoring points after NAC. Finally, the changes of BPE after 2nd and 4th NAC were independent variables correlated with better tumor response in the multivariate analysis, while the reductions of tumor size in each 3 monitoring points were independent variables correlated with pCR. The HR negative status was independent variable associated with pCR (Table 3).

Discussion

Of 90 patients with unilateral breast cancer in our study, the change of BPE in contralateral normal breast was firstly found to be correlated with the change of tumor size and patients with more reduction of BPE after 2nd NAC had more favorable pCR especially in HR-negative status. Similar to the previous studies, the BPE showed a constant reduction during the whole NAC.

Partially in line with previous studies, a significant decreased BPE was found during the whole NAC despite the menopausal status in this study. Previous studies analyzed the change of BPE after NAC in both pre-and post-menopausal status, in which 55 years or less was arbitrarily believed as pre-menopausal. In those studies, the reduction of BPE was only found in the pre-menopausal women [16,21,22]. The possible explanation for the results mainly in pre-menopausal women was chemotherapy-induced ovarian suppression [22]. BPE may demonstrate normal breast epithelial cell proliferation, which was affected by decreased hormone level due to ovarian suppression caused by NAC. To our knowledge, a direct damage of vessels in normal tissues, which contributed to the loss of tissue proliferation, may also cause a reduction in BPE regardless the menopausal status [23]. That could be explained that a significant decreased BPE was also found in post-menopausal women. As BPE may be sensitive to the hormonal changes, the reduction of BPE after NAC was less in post-menopausal women than that in pre-menopausal women in this study. Unlike in other studies, we focused on the change of BPE and size during every monitoring point in this study. BPE showed a constant reduction throughout chemotherapy and it fell down most obviously after the 2nd cycle, which was caused by the delivery of the therapeutic agent at the early stage of NAC.

To our knowledge, this is the first study to quantitatively investigate the relationship between BPE and tumor size on MRI throughout chemotherapy. Of relevance, RECIST standard is internationally agreed to influence treatment decisions and monitor tumor response during chemotherapy [20]. Some studies compared the clinical tumor size as assessed by MRI with the postoperative pathologic tumor size and revealed that tumor size on MRI had the ability to predict final tumor response at pathology during NAC [24,25]. Given the previous relevant findings that the alternation of BPE can also predict tumor outcome to NAC, the change of BPE may be similar to that of tumor size on the whole NAC. In our study, there was no correlation between BPE and tumor size in the baseline status at first, and it could be a hint towards other influences of tumor

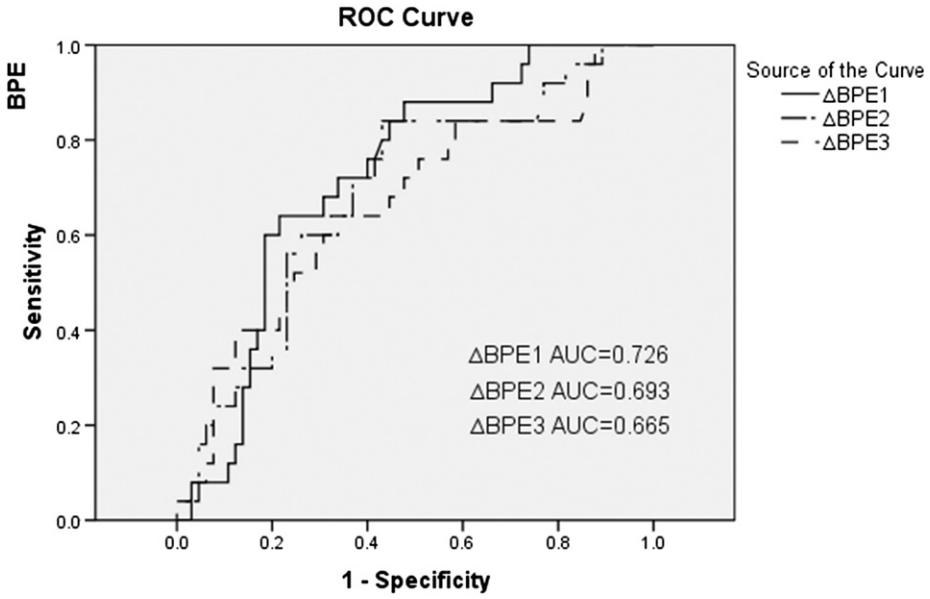

Figure 3. Receiver operating characteristics (ROC) analysis of BPE for the prediction of pathologic complete response (pCR). Note: $\Delta BPE_{1/2/3} = (BPE_{2nd/4th/6th\ follow\text{-}up\ MRI} - BPE_{baseline\ MRI})/BPE_{baseline\ MRI} *100\%$.

size preoperatively, which demonstrated that the initial tumor size did not predict tumor response [26]. However, the correlation between BPE and tumor size became weak but significant after NAC since both of them were affected by the therapeutic agent. Furthermore, it was also found that the reduction of BPE was positively correlated with the decrease of tumor size at every monitoring point. Because of the low *r* value in our exploratory study, larger investigations are warranted to fully examine the relationship between them.

Although a few studies have reported a high association between BPE and tumor outcome after NAC, they did not assess at multiple monitoring points throughout NAC. The measurements of BPE varied from previous quantitative analysis, such as the early phase of BPE, the mean value, and the differences in ration of BPE, and we calculated the mean value of BPE in this study. Our findings were in line with previous results, strongly suggesting that the reduction of BPE was associated with tumor response throughout NAC [15–17]. As we mentioned that BPE and tumor size had a similar tendency during NAC, both of them may therefore be sensitive to the effect of chemotherapy that had a positive prognostic value. From the ROC analysis, it was found that not only tumor size but also BPE could predict tumor response at every monitoring point in our study. The reduction of BPE was best at the early stage for predicting pCR, while the shrink of tumor size was best at the late stage as a predictor tool for pCR. More interestingly, both of them can serve as an early predictor

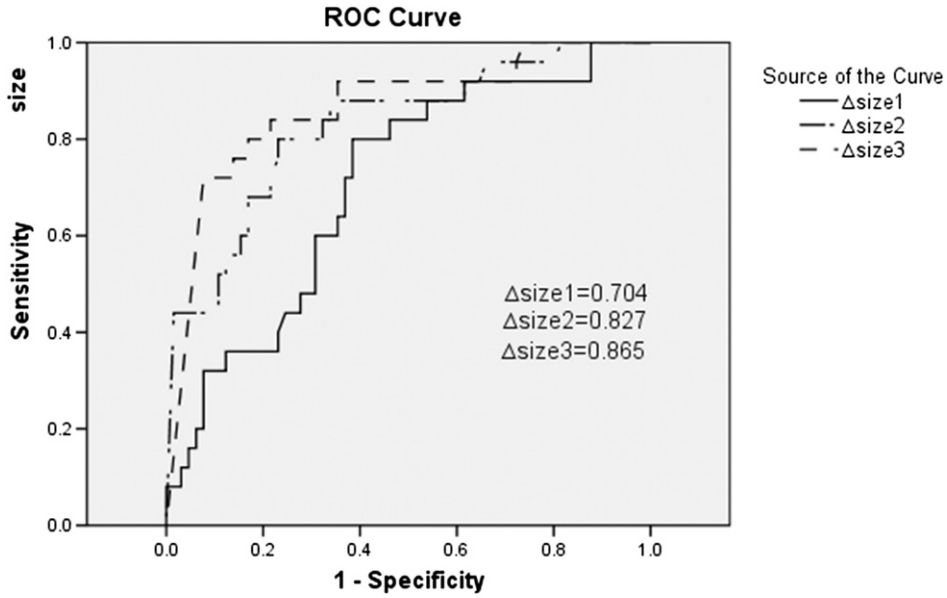

Figure 4. Receiver operating characteristics (ROC) analysis of size for the prediction of pathologic complete response (pCR). Note: $\Delta Size_{1/2/3} = (\text{tumor size}_{2nd/4th/6th\ follow\text{-}up\ MRI} - \text{tumor size}_{baseline\ MRI})/\text{tumor size}_{baseline\ MRI} *100\%$.

Table 2. Comparisons of AUC for the Discrimination of Δsize and ΔBPE

AUC	Area	*P*	95% CI	Cut-off Point	Sensitivity	Specificity
ΔBPE1	0.726	.001	0.618–0.835	0.2672	88%	52.3%
ΔBPE2	0.690	.005	0.569–0.811	0.4656	72%	63.1%
ΔBPE3	0.665	.016	0.536–0.794	0.6407	64%	67.7%
Δsize1	0.704	.003	0.588–0.821	0.3258	80%	61.5%
Δsize2	0.827	.000	0.729–0.925	0.6340	80%	76.9%
Δsize3	0.865	.000	0.776–0.954	0.6954	84%	78.5%

Note: $\Delta Size_{1/2/3}$ = (tumor $size_{2nd/4th/6th\ follow\text{-}up\ MRI}$ − tumor $size_{baseline\ MRI}$)/tumor $size_{baseline\ MRI}$ *100%. $\Delta BPE_{1/2/3}$ = ($BPE_{2nd/4th/6th\ follow\text{-}up\ MRI}$ − $BPE_{baseline\ MRI}$)/$BPE_{baseline\ MRI}$ *100%. OR = odds ratio. CI = confidence interval values.

tool for tumor response, but the ROC area of BPE was a little bit higher than tumor size after the 2nd cycle of NAC.

There have been only a few studies to investigate the association between BPE and tumor response stratified by IHC status, but the findings were not in complete unanimity. In our study, HR status was an independent variable associated with pCR, and the change of BPE after 2nd cycles showed a larger magnitude in HR-negative patients, which was partially in line with Chen's findings [16]. Since the HR-negative tumors were sensitive to chemotherapy and the HR-positive tumors benefit from endocrine therapy [27], the possible explanation of our findings was that the BPE may be more sensitive to the influence of blood perfusion resulting from chemotherapy agent than the effect of ovarian function affecting the hormonal level at the early stage after NAC. However, van der Velden et al. demonstrated the relatively different result that BPE was especially associated with long-term outcome in ER-positive and HER2-negative breast cancers[17]. Additionally, HER2 status showed significant association with pCR in univariate analysis but not an independent predictive factor in our findings. This warrants further investigations.

Our study has some limitations. First, because all of the patients had biopsy-proven breast cancer, MRI was not always performed in the recommended menstrual cycle in order to avoid a delay in treatment. Second, because only 12 patients received eight cycles of NAC, the evaluation of the 8th follow-up MRI was excluded in this study. Third, the population size is relatively small, and our population included only a small number of patients with pCR. Validation in larger populations is required to better explain the change of BPE on the whole NAC.

In conclusion, we demonstrated that BPE of contralateral normal breast showed a constant reduction throughout NAC therapy regardless of menopausal status, and the change of BPE was significantly correlated with the change of tumor size during the therapy. Furthermore, the reduction of BPE at the early stage (after 2nd cycle of NAC in this study) was firstly found to be positively associated with tumor response, particularly in HR-negative patients.

Table 3. Multivariate Analysis Between Variables and pCR After Receiving NAC

Variables		OR	95% CI	*P*
HR status	0	1.00(Reference)	-	-
	1	0.243	0.083–0.706	.009
HER2 status	0	1.00(Reference)		
	1			.099
Δsize1		0.069	0.006–0.835	.036
Δsize2		0.002	0–0.038	<.001
Δsize3		0	0–0.019	<.001
ΔBPE1		0.019	0.002–0.218	.002
ΔBPE2		0.033	0.002–0.590	.002
ΔBPE3		0.062	0.002–1.090	.111

Conflicts of Interest

None declared.

Grant Support

This project was supported (in part) by the grants from Shanghai Development Center for Construction Foundation of Clinical Supportive Department (Grant NO. SHDC22015030) and the National Natural Science Foundation of China (Grant No. 81301282 and 81,471,662).

Authors' Contributions

All authors contributed fundamentally to this study and participated sufficiently to take public responsibility for its content. Chao You, Wenxiang Zhi, and Guangyu Liu collected the data and were responsible for quality control of data and interpretation. Xuxia Shen reviewed all the pathologic specimens and collected the pathologic images. Luan Jiang was involved in the fully automated scheme for the quantitative analysis of BPE. Chao You, Li Xie, and Xiaoxin Hu were involved in the statistical analysis. Weijun Peng reviewed and edited the manuscript. Chao You wrote the manuscript. Yajia Gu edited and finalized the manuscript. Publication is approved by all authors.

Association between background parenchymal enhancement and pathologic complete remission throughout the neoadjuvant chemotherapy in breast cancer patients.

Acknowledgments

We thank all the patients of this study for their participation. We greatly appreciate Min Qian, Jian Mao, and Lei Yue at Department of Radiology for their excellent assistance.

References

[1] Morris EA, Comstock C, Lee C, and Lehman CD (2013). BI-RADS: magnetic resonance imaging 2013. In: D'Orsi CJ, Sickles EA, Mendelson EB, et al, editors. Breast Imaging Reporting and Data System: ACR BI-RADS, breast imaging atlas. Reston, Va: American College of Radiology; 2013.

[2] Wu S, Weinstein SP, DeLeo MR, Conant EF, Chen J, Domchek SM, and Kontos D (2015). Quantitative assessment of background parenchymal enhancement in breast MRI predicts response to risk-reducing salpingo-oophorectomy: preliminary evaluation in a cohort of BRCA1/2 mutation carriers. *Breast Cancer Res* **17**, 67.

[3] King V, Brooks JD, Bernstein JL, Reiner AS, Pike MC, and Morris EA (2011). Background parenchymal enhancement at breast MR imaging and breast cancer risk. *Radiology* **260**, 50–60.

[4] Kuhl CK, Bieling HB, Gieseke J, Kreft BP, Sommer T, Lutterbey G, and Schild HH (1997). Healthy premenopausal breast parenchyma in dynamic contrast-enhanced MR imaging of the breast: normal contrast medium enhancement and cyclical-phase dependency. *Radiology* **203**, 137–144.

[5] Ellis RL (2009). Optimal timing of breast MRI examinations for premenopausal women who do not have a normal menstrual cycle. *AJR Am J Roentgenol* **193**, 1738–1740.

[6] King V, Gu Y, Kaplan JB, Brooks JD, Pike MC, and Morris EA (2012). Impact of menopausal status on background parenchymal enhancement and fibroglandular tissue on breast MRI. *Eur Radiol* **22**, 2641–2647.

[7] Dontchos BN, Rahbar H, Partridge SC, Korde LA, Lam DL, Scheel JR, Peacock S, and Lehman CD (2015). Are Qualitative Assessments of Background Parenchymal Enhancement, Amount of Fibroglandular Tissue on MR Images, and Mammographic Density Associated with Breast Cancer Risk? *Radiology* **276**, 371–380.

[8] Telegrafo M, Rella L, Stabile IA, Angelelli G, and Moschetta M (2016). Breast MRI background parenchymal enhancement (BPE) correlates with the risk of breast cancer. *Magn Reson Imaging* **34**, 173–176.

[9] Kim JY, Kim SH, Kim YJ, Kang BJ, An YY, Lee AW, Song BJ, Park YS, and Lee HB (2015). Enhancement parameters on dynamic contrast enhanced breast MRI: do they correlate with prognostic factors and subtypes of breast cancers? *Magn Reson Imaging* **33**, 72–80.

[10] Kim SA, Cho N, Ryu EB, Seo M, Bae MS, Chang JM, and Moon WK (2014). Background parenchymal signal enhancement ratio at preoperative MR imaging: association with subsequent local recurrence in patients with ductal carcinoma in situ after breast conservation surgery. *Radiology* **270**, 699–707.

[11] Choi JS, Ko ES, Ko EY, Han BK, and Nam SJ (2016). Background parenchymal enhancement on preoperative magnetic resonance imaging: association with recurrence-free survival in breast cancer patients treated with neoadjuvant chemotherapy. *Medicine (Baltimore)* **95**, e3000.

[12] Pfleiderer SO, Sachse S, Sauner D, Marx C, Malich A, Wurdinger S, and Kaiser WA (2004). Changes in magnetic resonance mammography due to hormone replacement therapy. *Breast Cancer Res* **6**, R232-38.

[13] King V, Goldfarb SB, Brooks JD, Sung JS, Nulsen BF, Jozefara JE, Pike MC, Dickler MN, and Morris EA (2012). Effect of aromatase inhibitors on background parenchymal enhancement and amount of fibroglandular tissue at breast MR imaging. *Radiology* **264**, 670–678.

[14] King V, Kaplan J, Pike MC, Liberman L, David DD, Lee CH, Brooks JD, and Morris EA (2012). Impact of tamoxifen on amount of fibroglandular tissue, background parenchymal enhancement, and cysts on breast magnetic resonance imaging. *Breast J* **18**, 527–534.

[15] Preibsch H, Wanner L, Bahrs SD, Wietek BM, Siegmann-Luz KC, Oberlecher E, Hahn M, Staebler A, Nikolaou K, and Wiesinger B (2016). Background parenchymal enhancement in breast MRI before and after neoadjuvant chemotherapy: correlation with tumour response. *Eur Radiol* **26**, 1590–1596.

[16] Chen JH, Yu HJ, Hsu C, Mehta RS, Carpenter PM, and Su MY (2015). Background parenchymal enhancement of the contralateral normal breast: association with tumor response in breast cancer patients receiving neoadjuvant chemotherapy. *Transl Oncol* **8**, 204–209.

[17] van der Velden BH, Dmitriev I, Loo CE, Pijnappel RM, and Gilhuijs KG (2015). Association between parenchymal enhancement of the contralateral breast in dynamic contrast-enhanced MR imaging and outcome of patients with unilateral invasive breast cancer. *Radiology* **276**, 675–685.

[18] Ogston KN, Miller ID, Payne S, Hutcheon AW, Sarkar TK, Smith I, Schofield A, and Heys SD (2003). A new histological grading system to assess response of breast cancers to primary chemotherapy: prognostic significance and survival. *Breast* **12**, 320–327.

[19] Hu X, Jiang L, Li Q, and Gu Y (2017). Quantitative assessment of background parenchymal enhancement in breast magnetic resonance images predicts the risk of breast cancer. *Oncotarget* **8**, 10620–10627.

[20] Therasse P, Arbuck SG, Eisenhauer EA, Wanders J, Kaplan RS, Rubinstein L, Verweij J, Van Glabbeke M, van Oosterom AT, and Christian MC, et al (2000). New guidelines to evaluate the response to treatment in solid tumors. European Organization for Research and Treatment of Cancer, National Cancer Institute of the United States, National Cancer Institute of Canada. *J Natl Cancer Inst* **92**, 205–216.

[21] Chen JH, Yu H, Lin M, Mehta RS, and Su MY (2013). Background parenchymal enhancement in the contralateral normal breast of patients undergoing neoadjuvant chemotherapy measured by DCE-MRI. *Magn Reson Imaging* **31**, 1465–1471.

[22] Swain SM, Jeong JH, Geyer CE, Costantino JP, Pajon ER, Fehrenbacher L, Atkins JN, Polikoff J, Vogel VG, and Erban JK, et al (2010). Longer therapy, iatrogenic amenorrhea, and survival in early breast cancer. *N Engl J Med* **362**, 2053–2065.

[23] Miller Kathy D, Sweeney Christopher J, and Sledge Jr George W (2001). Redefining the target: chemotherapeutics as antiangiogenics. *J Clin Oncol* **19**, 1195–1206.

[24] Bhattacharyya M, Ryan D, Carpenter R, Vinnicombe S, and Gallagher CJ (2008). Using MRI to plan breast-conserving surgery following neoadjuvant chemotherapy for early breast cancer. *Br J Cancer* **98**, 289–293.

[25] Charehbili A, Wasser MN, Smit VT, Putter H, van Leeuwen-Stok AE, Meershoek-Klein KW, Liefers GJ, van de Velde CJ, Nortier JW, and Kroep JR (2014). Accuracy of MRI for treatment response assessment after taxane- and anthracycline-based neoadjuvant chemotherapy in HER2-negative breast cancer. *Eur J Surg Oncol* **40**, 1216–1221.

[26] Ko ES, Han BK, Kim RB, Ko EY, Shin JH, Hahn SY, Nam SJ, Lee JE, Lee SK, and Im YH, et al (2013). Analysis of factors that influence the accuracy of magnetic resonance imaging for predicting response after neoadjuvant chemotherapy in locally advanced breast cancer. *Ann Surg Oncol* **20**, 2562–2568.

[27] Cortazar P, Zhang L, Untch M, Mehta K, Costantino JP, Wolmark N, Bonnefoi H, Cameron D, Gianni L, and Valagussa P, et al (2014). Pathological complete response and long-term clinical benefit in breast cancer: the CTNeoBC pooled analysis. *Lancet* **384**, 164–172.